Feasibility Study of a Wide Coverage Dual-Polarized Phased Array Antenna at 10 GHz

Feasibility Study of a Wide Coverage Dual-Polarized Phased Array Antenna at 10 GHz

Prabhat Khanal[1], Jian Yang[1], Marianna Ivashina[1]
[1] Department of Electrical Engineering, Chalmers University of Technology, Gothenburg, Sweden
prabhat@chalmers.se, jian.yang@chalmers.se, marianna.ivashina@chalmers.se

***Abstract*—The paper studies the feasibility of designing and manufacturing a low-profile, dual-polarized wide-scan X-band (10 GHz) antenna array. In a large array environment, approximated as an infinitely large array, the antenna is capable of beam scanning up to $\pm 75^\circ$ with a bandwidth of 15% in terms of the active reflection coefficient (Γ_{act}) below -10 dB.**

***Index Terms*—Bowtie antenna array, connected antenna array, phased array, wide scan, x-band.**

I. Introduction

Phased array antennas are capable of steering their antenna beam electronically. They are more flexible and capable of high-speed beam scan compared to mechanically beam steering antennas. Therefore, phased array antennas are widely used nowadays in communication and radar applications. However, unlike mechanical beam steering antennas, phased array antennas have limitations on their beam steering (scanning) range. For wide scan angles, the scan impedance deteriorates depending on the inter-element separation distance and the number of antenna elements [1].

Connected antenna element arrays represent a suitable solution for wide-scanning applications [2]. This concept has been used for dipole [2], Vivaldi [3] and slot [4] antenna elements. This paper presents a connected cross-bowtie element that is capable of beam steering upto $\pm 75^\circ$ at X-band (10 GHz) with the bandwidth of 15% and active reflection coefficient ($|\Gamma_{act}|$)) ≤ -10 dB in an infinitely large antenna array.

II. Antenna design

Fig. 1 shows a unitcell of the cross-bowtie antenna element and its cross-section view. Fig. 2 shows the antenna array assembly for an example of a 3×3 connected cross-bowtie antenna elements. The antenna element is based on the previous cross-bowtie antenna element design which operates at S-band [5]. Simple geometrical scaling of the antenna element from S-band to X-band is not possible to realize. One need to re-optimize the antenna element according to the manufacturing feasibility at X-band. The geometrical parameters of the antenna element (shown in Fig. 1a) are given in TABLE I.

An antenna element has three parts: a) ground plane with two solid metal pillars, b) a PCB with the radiating antenna element and c) two standard $50\,\Omega$ RF coaxial connector with the extended coaxial cable. The PCB consists of two orthogonal bowtie elements and is placed above two solid pillars which are connected via screw threads to the ground plane. The coaxial cable is inserted from the underside of the ground plane through the holes in the ground plane. The outer conductor of the coaxial cable is connected to the ground plane at one end and to one of the arms of a bowtie pair at another end. The inner conductor of the coaxial cable is connected to

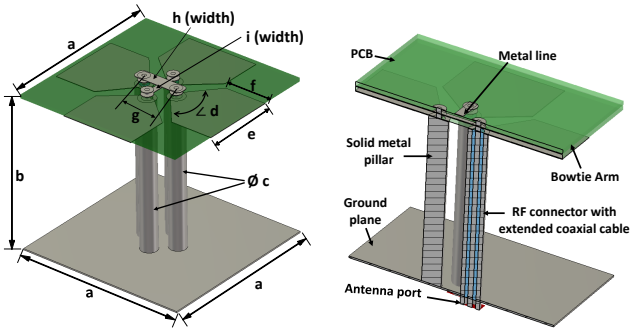

(a) Antenna parameters (b) Corss-section view

Fig. 1: Unitcell of the cross-bowtie antenna element.

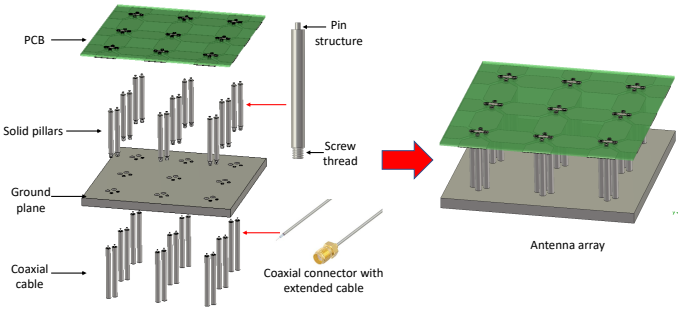

Fig. 2: Antenna array assembly with the extended coaxial cable for an example of a 3×3 connected cross-bowtie antenna elements

TABLE I: Geometrical parameters of the optimized cross-bowtie antenna element as defined in Fig. 1a.

Parameter	Value [mm]	Parameter	Value [mm]
a	12	g	2.5
b	10.5	h	0.9
c	1.2	i	0.4
d	98.6°	$D_i^\dagger$	0.3
e	5.2	$D_o^\dagger$	0.7
f	3		

† Parameters D_i and D_o are diameters of the inner conductor and the dielectric layer of the extended coaxial cable.

the other arm of the same bowtie (where the outer conductor of the coaxial cable is connected) through a metal line on the top layer of the PCB. The solid pillar is connected to this arm at one end and to the ground plane at another. Similarly, another pair of a coaxial cable and a solid pillar is connected to the other pair of the bowtie for second polarization. The metal line for the second pair of coaxial cable and solid pillar goes from the middle layer of the PCB. The solid pillar, the coaxial cable and the metal line function as a folded balun transforming single-ended antenna input port to a differential port of the bowtie elements. The unitcell has the volume of $d_x \times d_y \times d_z$ = $0.4\lambda \times 0.4\lambda \times 0.34\lambda$, where λ corresponds to the wavelength in free-space at 10 GHz. The PCB stack-up is copper (35μm) – substrate (254μm) – copper (35μm) – substrate (254μm) – copper (35μm), where the substrate is Rogers 4350B. The antenna element is designed for a connected array structure to maximize wide scan angle capabilities.

The antenna array assembly is shown in Fig. 2. The PCB and the ground plane can be manufactured as a single piece for the entire antenna array using a standard PCB manufacturing process and CNC metal machining respectively. The coaxial connector with the extended semi-rigid coaxial cable is a standard RF connector and can be bought from an electronics parts retailer. The solid pillars can be manufactured individually using CNC metal machining as well. The solid pillars would have screw threads on the bottom side and can be screwed to the ground plane in order to make the ground and solid pillar structures. After assembling the ground plane and solid pillars, the PCB is placed on top of it and soldered with the pin structures on top of the solid pillars. Finally, the coaxial connector with the coaxial cable would be inserted and its inner connector is soldered on the top layer of the PCB.

III. Simulation Results

The antenna array is excited with uniform amplitude and a linear phase progression to steer its main beam in different directions. The antenna element was simulated using an infinite array model. Fig. 3 shows the active reflection coefficient for horizontal and vertical polarized antenna elements in E-plane. Herein, we can see that the antenna element is capable of beam scanning up to $\pm 75^\circ$ with the active reflection coefficient ($|\Gamma_{act}|$) of ≤ -10dB with the bandwidth of 15%. Notice that for both polarizations, the active reflection coefficients are centred at 10 GHz. This was achieved by making the stripline (see Fig. 1a) in the middle layer of the PCB narrower than the microstrip line which is on the top layer of the PCB.

Fig. 4 shows the antenna gain patterns of the 64×64 connected cross-bowtie antenna element array. The main beam of the antenna array is steered in [0°, 75°] scan angle range in both polarizations. Maximum gain at the broadside is 39 dBi and it decreases to 33 dBi at scan angle 75°. The sidelobe level at broadside is −13.3 dB and it increases to −10.8 dB at scan angle 75°. The decrease in the maximum gain and the increase in the sidelobe levels is due to the combined effect of the scan loss and finiteness of the antenna array. The array is symmetric and it performs in the same way in [−75°,0°] scan range as it performs in [0°, 75°] scan range. The radiation efficiency of the antenna element η_{rad} ≥98% for the 15% bandwidth across the $\pm 75^\circ$ scan range.

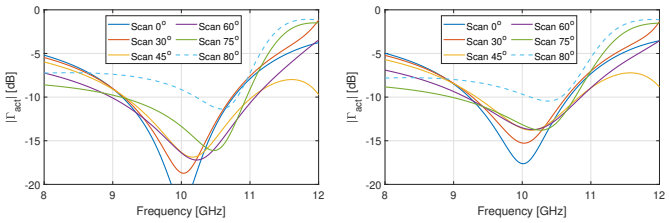

(a) Horizontal polarization (b) Vertical polarization

Fig. 3: The active reflection coefficients of the cross-bowtie antenna element in the infinitely large array.

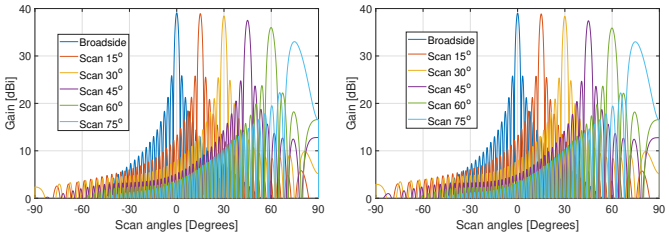

(a) Horizontal polarization (b) Vertical polarization

Fig. 4: Antenna gain patterns of the 64×64 connected cross-bowtie element array when steering its main beam in E-plane at 10 GHz.

IV. Conclusion

The paper shows the manufacturing feasibility to realize the wide scanning cross-bowtie antenna element array at 10 GHz. Both horizontal and vertical polarized elements show promising results. The active reflection coefficient and radiation pattern of the unitcell shows the scanning capabilities up to $\pm 75^\circ$ with the bandwidth of 15% and $|\Gamma_{act}| \leq -10$ dB as expected.

References

[1] D. Pozar and D. Schaubert, "Scan blindness in infinite phased arrays of printed dipoles," *IEEE Transactions on Antennas and Propagation*, vol. 32, no. 6, pp. 602–610, 1984.

[2] D. Cavallo, G. Gerini, R. Bolt, D. Deurloo, R. Grooters, A. Neto, G. Toso, and R. Midthassel, "Ku-band dual-polarized array of connected dipoles for satcom terminals: Theory and hardware validation," in *2013 7th European Conference on Antennas and Propagation (EuCAP)*, pp. 459–460, April 2013.

[3] R. Maaskant, M. V. Ivashina, O. Iupikov, E. A. Redkina, S. Kasturi, and D. H. Schaubert, "Analysis of large microstrip-fed tapered slot antenna arrays by combining electrodynamic and quasi-static field models," *IEEE Transactions on Antennas and Propagation*, vol. 59, pp. 1798–1807, June 2011.

[4] D. Cavallo, W. H. Syed, and A. Neto, "Connected-slot array with artificial dielectrics: A 6 to 15 ghz dual-pol wide-scan prototype," *IEEE Transactions on Antennas and Propagation*, vol. 66, pp. 3201–3206, June 2018.

[5] P. Khanal, J. Yang, M. Ivashina, A. Hook, and R. Luo, "A wide coverage s-band array with dual polarized connected bowtie antenna elements," in *2019 IEEE International Symposium on Antennas and Propagation and USNC-URSI Radio Science Meeting*, pp. 2001–2002, 2019.